Mechanical Systems and Signal Processing 165 (2022) 108318

Contents lists available at ScienceDirect

Mechanical Systems and Signal Processing

journal homepage: www.elsevier.com/locate/ymssp

A study on spot welding quality judgment based on improved generative adversarial network and auto-encoder

Bing Wang [a,b]

[a] College of Mathematics and Statistics, Chongqing Technology and Business University, Chongqing 400067, China
[b] Chongqing Key Laboratory of Social Economy and Applied Statistics, Chongqing 400067, China

ARTICLE INFO

Keywords:
Generative adversarial network
Auto-encoder
HMM
Spot welding
Quality judgment

ABSTRACT

To address the problems that only a few unqualified spot welding joint samples are obtained during spot welding, and traditional feature extraction methods are unable to obtain hidden deep-seated quality features of spot welding, an improved method was proposed in this paper to judge the spot welding quality. The proposed method integrated the generative adversarial network (GAN) and the auto-encoder (AE) to construct a network structure having the functions of sample data generation, feature extraction and pattern recognition. It also presented appropriate improvements to address the insufficient diversification of generated samples in the standard GAN. An improved generative adversarial network (IGAN) was first employed to expand the samples dataset of unqualified spot welding joints, which was followed by the selection of feature vector of the samples through AE combined with personal experience. A hidden Markov model (HMM) was utilized at the end to judge the spot welding quality. The spot welding joint samples data of stainless steel railway carriage roof were employed in this study to prove that the proposed improved method is feasible. It ensured that the generated data can fit the waveform curve of spot welding joint samples with unqualified quality as far as possible, at the same time, spent shorter time for training and testing data sets and provided a higher classification accuracy than other classification methods.

1. Introduction

Resistance spot welding (hereinafter referred to as spot welding) is a basic practice for workpiece connection, quality of which directly affects the structure usability. Therefore, it is crucial to evaluate the spot welding quality. Spot welding, however, is a complex process characterized by high nonlinearity, multivariable coupling and a large number of random uncertainties interacting with each other, in which any short-term fluctuation of welding conditions will cause serious consequences e.g. spatter, incomplete penetration and unfused [1].

Around this problem, scholars in China and overseas have carried out a series of research, such as, Podrzaj et al. [2] presented an overview of resistance spot welding control. Zhou et al. [3] presented recent primary advances and progress in process analysis and quality control of the RSW operations. Kimchi et al. [4] in lecture "Resistance Spot Welding: Fundamentals and Applications for the Automotive Industry", described the basic principle of RSW, its contents included: welding piece, electrode force, contact resistance, dynamic resistance, heat balance, current waveform, nugget generation, etc. Al-Mukhtar [5] described the process and failure mode of RSW.

E-mail address: wangbing1783@sina.com.

https://doi.org/10.1016/j.ymssp.2021.108318
Received 21 January 2021; Received in revised form 21 June 2021; Accepted 3 August 2021
Available online 6 September 2021

Mallaradhya et al. [6] reviewed resistance spot welding with different materials, optimization techniques.

Through collation and analysis of relevant literatures, it is not difficult to find: non-destructive testing of spot welding quality, control of spot welding quality, monitor of RSW process in real-time, and welding of new materials still represent the directions and hot spots for research.

However, in the field of railway transport, many key components are not allowed to be dissected as a whole for inspection, while each spot welding joint has to be manually inspected, which adds to the difficulty of accurate detection of spot welding defects. A reliable and practical detection method is still not available for the spot welding quality now, because the extremely short nucleation time of spot welding does not allow direct observation. As a result, it is extremely urgent to judge the spot welding joints quality through monitoring the nugget size, metallurgical defects and joint strength stability in the process of spot welding.

In recent years, increasing attention has been paid to those studies that establish mathematical models between the dynamic parameters of the spot welding process and the nugget size to judge the spot welding quality. Common examples of these mathematical models include support vector machine [7–9], neural network [10–12], regression analysis [13–14], and HMM [15–17]. Such models are characterized by extracting features from the parameters closely related to the spot welding process and establishing mathematical models between the feature vector and the nugget size, tension-shearing strength of joints and other indicators to judge the spot welding quality and monitor the spot welding process. The limitations are:

(1) The classification accuracy of the model is affected by the number of spot welding joint samples. In view of this, the classification effect cannot be guaranteed for a data set with less samples. As the process parameters are constantly optimized and more rules are specified for the spot welding, the number of qualified spot welding joint samples obtained during spot welding is much more than the number of unqualified ones. However, traditional pattern classification methods depend on the learning of model parameters and are hard to obtain better model parameters by training through only a few unqualified spot welding joint samples, which greatly affects the subsequent pattern classification results.
(2) The feature extraction mostly depends on expert experience and there is no set pattern to follow. As a result, the number of selectable features is limited. Moreover, hidden deep-seated quality features of spot welding are difficult to be directly extracted during spot welding as a result of the closed state of nugget formation.

In view of these problems, a method for judging the spot welding quality based on a small sample data set was proposed in this paper, which has the following innovative points:

- For the problem (1), a GAN was employed in this paper to generate unqualified spot welding joint samples and expand the sample dataset until the number of each kind of unqualified spot welding joint samples turned almost the same with the number of qualified ones. Moreover, in view of the limitation of standard GAN algorithm, that is, there is no guarantee that each kind of unqualified spot welding joint samples has equal chances to generate its own samples, a corresponding improvement was also presented in this paper.
- For the problem (2), an AE was adopted to learn the features of both qualified and unqualified spot welding joint samples, so that with the assistance of personal experience, the feature vector set of each kind of spot welding joint samples could be obtained.

Further, an HMM classifier was used to judge the spot welding quality based on the acquired spot welding joint sample data. Sample data acquired from the spot welding process of stainless steel railway carriage roof was used in this study to prove that the proposed improved method is feasible, comparison of the other three classification methods, that's GAN-AE, AE and HMM, and the results manifested the proposed method was better in spot welding quality judgment.

This paper then introduced the theoretical basis of this study in Section 2, elaborated on the proposed method, verified the proposed method by virtue of experiments, and presented the conclusions at the end.

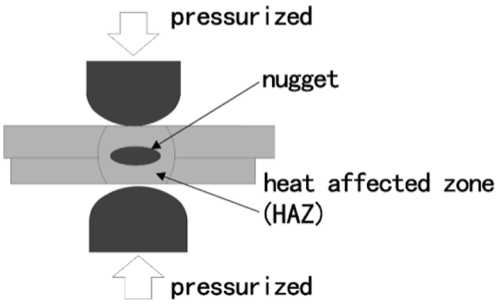

Fig. 1. Schematic diagram of resistance spot welding.

2. Theoretical basis

2.1. RSW's principle

Resistance welding is a pressure welding method that makes the current pass through the workpiece to be welded, uses the resistance heat as the heat source to melt the metal, and at the same time applies certain pressure to the workpiece so that the workpiece is connected. Its working principle is illustrated in Fig. 1.

There are three stages involved in the spot welding process to form the joint:

- Apply pressure. Electrodes are used to apply pressure, clamp and hold the work-pieces together without gap, and maintain the required electrical resistance during welding.
- Apply electric current to generate heat. The current passes through the contact surface, and the heat generated is used to heat the workpiece, thus reaching the molten state and forming the nugget.
- Cooling crystallization. After the electric current is turned off, the molten nugget solidifies. Then a big contraction is observed in the process of cooling crystallization. In this stage, a proper cooling time shall be defined and the pressure from the electrodes is maintained to get a more dense crystallization microstructure.

2.2. Generative adversarial network

A GAN is composed of a generative network$G$ and a discriminant network D and its structure is shown in Fig. 2. The basic idea of GAN is that the generative network transforms random noise into a real sample space, expecting the generated data to be distributed as real data, while the discriminant network can output the generated data as true; and the discriminant network is to distinguish between true and false inputs as far as possible, by judging the generated data as false and the real data as true. During the confrontation and competition, the two networks are both optimized with improved performance, and such optimization shall continue until the discriminant network cannot identify the data source any more.

For the generative network, the generated data$G(z)$ shall be as close as possible to the real data x; the discriminant network can give the confidence level of the input data deriving from the real data, that is, when the discriminant network inputs$x$, $D(x)$ is close to 1, while the input becomes $G(z)$, the value of $D[G(z)]$ is close to 0. Thus, the objective function of GAN in training is expressed as:

$$L_{GAN} = \min_{G}\left\{\max_{D}\{E(x \sim P_{data}(x)) \cdot [lnD(x)] + E(z \sim P_z(x)) \cdot [ln(1 - D(G(z)))]\}\right\} \tag{1}$$

As a generative model, the most direct application of GAN is data generation. Currently, GAN has been broadly applied in machine vision, image processing and other fields, but is relatively less used in welding process. Gu et al. [18] adopted the deep convolutional generative adversarial network to balance the dataset, aiming at solving the problem that the unbalanced numbers of welding defects affected the classification accuracy. Huang [19] achieved data enhancement for the weld defect learning samples based on a GAN. Nevertheless, the above researches have not proposed a desirable solution to address the limitations of GAN, such as difficult training and insufficient diversification of generated data.

2.3. Auto-encoder

AE is an unsupervised feature learning algorithm, its network consists of single input, single output and multiple hidden layers, among them, the hidden layer is used for encoding the input data, while the output layer is used for decoding the code to data. The encoders learn the low-dimensional features of input signals, whereas the decoder reproduces the input signals as far as possible. Hence, the ultimate goal of AE is to reconstruct its inputs so that the encoders can learn the good low-dimensional features of the inputs.

At present, the applications of AE in spot welding process include the classification of spot welding quality and the on-line monitoring of spot welding process, but AE is often combined with other models (e.g., GAN) to improve the performance, as AE has no classification ability and is difficult to determine the model parameters. Xiong et al. [20] proposed a method for fault diagnosis of rolling bearing, which integrated WGAN and SAE network. Wang et al. [21] applied CVAE and GAN in an example of unbalanced fault diagnosis. Chakraborety at al. [22] designed a novel Generative Adversarial based deep Autoencoder to classify datasets under normal and faulty operating conditions.

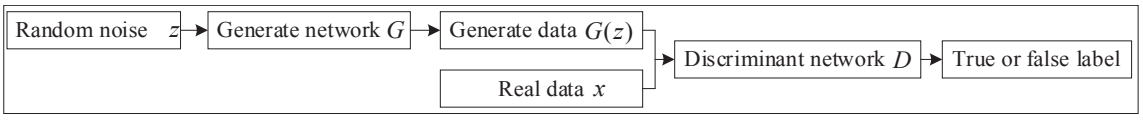

Fig. 2. GAN structure.

2.4. Research status analysis

The analysis of existing research results reveals that,

(1) Although using GAN to generate unqualified spot welding joint samples addresses the problem of data deficiency during model training, the generated samples in the GAN are lack of diversification. That is to say, after inputting the data of unqualified spot welding joint samples (unfused, small nugget, cracked, spatter etc.) into GAN, there is no guarantee that each spot welding joint sample has equal chances to generate its own samples. As a result, only one type or several types of samples would be generated. The root cause is that the random noise has fewer constraints and thus cannot better fit to the distribution of sample data of unqualified spot welding joints.
(2) Applying AE in the spot welding quality judgment avoids the over-reliance on personal experience during feature extraction to some extent, but the effectiveness of the obtained features has to be further verified. For example, if only the maximum spot welding current is selected as its feature, it would be difficult to judge the spot welding quality, as the maximum spot welding current of spot welding with unfused is close to that of spot welding with incomplete penetration in some cases.
(3) Integrating GAN with AE gives play to their advantages, namely using GAN to guarantee the quantity of samples and using AE to extract the features of samples. However, further study is required for the details, e.g. when to input the samples generated by GAN into AE; which are to be selected, the original samples or the features of samples, or taking a part of AE's network structure as the generator of GAN.

3. The proposed method

Based on existing research results and the limitations of GAN, a method combined GAN with AE was proposed in this paper for spot welding quality judgment, which was described in details in this section.

3.1. GAN improvement

In Section 2: Theoretical Basis of this paper, the problem of GAN is pointed out i.e. the insufficient diversification of generated data, which stems from the following facts:

- In the early stage of training, due to the low quality of data generated by the generator, the discriminator could easily distinguish the generated data from the real, so the generator has no optimized signal to use for self-optimization, nor could the model generate meaningful data.
- GAN utilizes the discriminator to judge the probability that the generated data are real and thus promotes the generator to learn, but it could not judge whether the generated data has sufficient diversification or not, so models with high probabilities would be more likely to be generated. Moreover, once the generator has learned the mode of how to generate high probability models, such models are highly prone to be generated constantly, which leads to mode collapse.

At present, most of the improvements solve these problems by adding restrictions, such as sample labels, or adding feedback adjustment layers, but rarely involve the adjustment of the generative network structure. In view of this, an improved method (named IGAN) was proposed in this paper, whose basic idea was to proportionally blend the generated and the real samples to obtain a mixture for substituting the generated samples in the standard GAN. This method could not only mitigate the difference between generated samples and rear samples and enhance the generation ability of the generator, but also ensure sufficient diversification for the generated data and avoid mode collapse to some extent. Its structure is shown in Fig. 3. Where the random noise z follows the Gaussian distribution; and α is the mixing proportion coefficient and its value is a real number in the interval $(0,1)$.

(1) Objective function

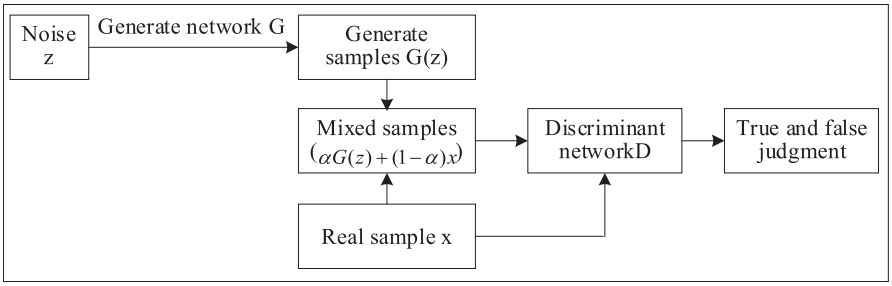

Fig. 3. IGAN structure.

Real sample data × originate from the signals that are obtained by sensors during spot welding, including welding current, inter-electrode voltage and electrode pressure. Random noise z is generated by simulating the noise made by the spot welding machine during working through a computer. In Fig. 3, $G(z)$ denotes the noise data generated using the generative network G, and $\alpha \cdot G(z) + (1-\alpha) \cdot x$ denotes a mixed sample obtained by mixing the data of process parameters collected during spot welding with the environmental noise data $G(z)$ at a certain ratio. Therefore, the objective function of IGAN can be expressed as:

$$L_{IGAN} = \min_{G}\left\{\max_{D}\left\{\begin{array}{c} E(x \sim P_{data}(x)) \cdot [lnD(x)] + \\ [\alpha \cdot E(z \sim P_z(x)) + (1-\alpha) \cdot E(x \sim P_{data}(x))][ln(1 - D(\alpha \cdot G(z) + (1-\alpha) \cdot x))] \end{array}\right\}\right\} \tag{2}$$

Therefore, when

$$D_G^*(x) = \frac{P_{data}(x)}{(2-\alpha)P_{data}(x) + \alpha P_z(x)} \tag{3}$$

Equation (2) reaches the maximum. In Equation (3), $P_{data}(x)$ denotes the distribution of obtained data of process parameters (welding current, inter-electrode voltage, electrode pressure, etc.), and $\boldsymbol{P}_z(x)$ denotes the environmental noise, which obeys uniform or normal distribution. When the distribution $P_z(x)$ of environmental noise data is infinitely close to the distribution $P_{data}(x)$ of process parameter data i.e. $P_{data}(x) = P_z(x)$, the discriminator is $D_G^*(x) = 1/2$ and G is the global optimal solution. According to the above Equations,

- When $\alpha \to 1$, Equation (3) degenerates to the condition that the objective function of the standard GAN reaches the maximum, in which case,

$$D_G^*(x) = \frac{P_{data}(x)}{P_{data}(x) + P_z(x)} \tag{4}$$

It demonstrates that the standard GAN can be regarded as a particular case of IGAN.

- The conditions for an IGAN to obtain its global optimal solution are same with those of a GAN. According to the existing theoretical derivation results [23], the improved method proposed in this paper can also ensure an IGAN to obtain the global optimal solution, proving the theoretical feasibility of the proposed method.

(2) Network training

The IGAN network consists of two parts i.e. obtaining the optimal values of D and G by $max(G,D)$ and $min(G,D)$, respectively.

- Training of the discriminator D

Equation (2) manifests that the mathematical expectations $E(z \sim P_z(x))$ and $E(x \sim P_{data}(x))$ of the generated data $P_z(x)$ and the real data $P_{data}(x)$, respectively, have to be obtained first to solve D. Nevertheless, the two expectations can not be solved out by integral operations in practice, so sampling from the real data and the generated data was performed in this study separately to approximate the expectations. The specific process is as follows:

Step1. Sampled m samples $\{x_1, \cdots, x_m\}$ from the real data $P_{data}(x)$.

Step 2. Sampled m samples $\left\{\widetilde{x}_1, \cdots, \widetilde{x}_m\right\}$ from the random noise data $P_z(x)$.

Step 3. Calculate the sampling value of real sample data $E(x \sim P_{data}(x)) \cdot [lnD(x)]$, that is $\frac{1}{m} \cdot \sum_{i=1}^{m} ln[D(x_i)]$.

Step 4. Calculate the sampling value of mixed sample data: $[\alpha \cdot E(z \sim P_z(x)) + (1-\alpha) \cdot E(x \sim P_{data}(x))] \cdot [ln(1 - D(\alpha \cdot G(z) + (1-\alpha) \cdot x))]$, that is $\left[\alpha \cdot \frac{1}{m} + (1-\alpha) \cdot \frac{1}{m}\right] \sum_{i=1}^{m} ln\left[1 - D(\alpha \cdot \widetilde{x}_i + (1-\alpha) \cdot x_i)\right] = \frac{1}{m} \cdot \sum_{i=1}^{m} ln\left[1 - D(\alpha \cdot \widetilde{x}_i + (1-\alpha) \cdot x_i)\right]$.

At this time,

$$max\{G,D\} \approx \frac{1}{m} \cdot \sum_{i=1}^{m} ln[D(x_i)] + \frac{1}{m} \cdot \sum_{i=1}^{m} ln\left[1 - D\left(\alpha \cdot \widetilde{x}_i + (1-\alpha) \cdot x_i\right)\right] \tag{5}$$

- Training of the generator G

After training the discriminator D, G could be obtained through $min(G,D)$.

Because the generative network$G$and the discriminant network $D$are both differentiable functions, because the gradient descent algorithm has the advantages of simple implementation and fast convergence, so it was employed to update the parameters, and the steps are shown in Fig. 4.

(3) Model evaluation

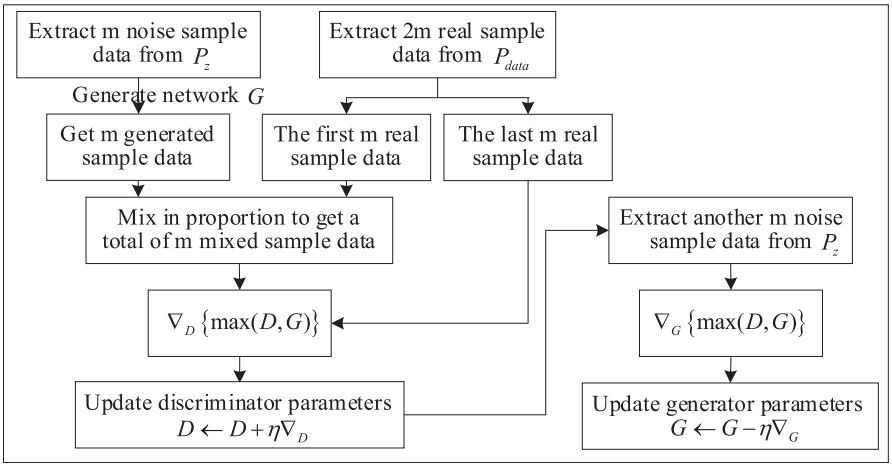

Fig. 4. IGAN parameter update process.

Qualitative evaluation was combined with quantitative evaluation in this paper and appropriate evaluation criteria were selected adaptive to specific tasks, as described below:

Visual inspection is a common method to qualitatively evaluate the spot welding quality, but considering the influence of subjective perception, cognitive level and other factors on the evaluation results, non-subjective quantitative evaluation methods remain necessary. In other words, an AE for judging the spot welding quality was trained first according to the monitored waveforms of spot welding quality under different states to obtain the feature vector sets of different quality states. Then the real-time monitored sample data with the state unknown were used for testing. At last, an HMM was employed to calculate the logarithmic likelihood probability and thus judge whether the spot welding joint quality was qualified or not.

3.2. IGAN and AE method for judging spot welding quality

(1) Basic idea

To address the problem of less unqualified spot welding joint samples when welding the stainless steel carriage roof, a spot welding quality judgment method was put forward in this study, which integrated IGAN with AE (referred to as IGAN-AE). The basic idea of this method is as follows: the IGAN was first employed to generate unqualified spot welding joint samples and thus let the number of spot welding joint samples roughly keep the same under different spot welding quality states; then the sample data of each type of spot welding joint were normalized and input into an AE to obtain the corresponding feature vectors of different states, while the features were selected based on personal experience to determine the final feature vector set; and at last, the feature vector set and the test samples were input into an HMM to obtain the judgment results of spot welding quality. The implementation process of this method is illustrated in Fig. 5.

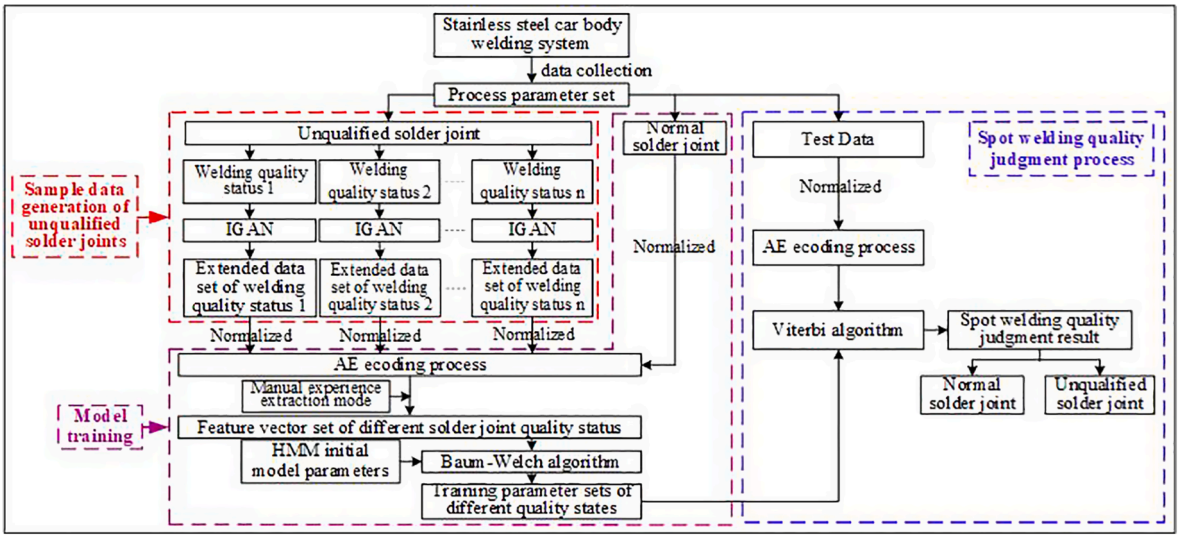

Fig. 5. Spot welding quality judgment process based on IGAN and AE.

(2) Implementation

◆ Sample data generation of unqualified spot welding joints

Sensors of current, voltage, pressure, etc. were installed on a spot welding machine to acquire the current, voltage, interelectrode pressure and other data during spot welding and generate the sample data of unqualified spot welding joints. Specific steps were as follows: for each quality state of unqualified spot welding joints, m noise data were first extracted from the stochastic noise z, and then m noise sample data were generated via the generative network$G$. Afterwards, the waveforms of unqualified spot welding joints, including unfused, small nugget, cracked and spatter etc., were sampled to collect $2m$ samples for each quality state. The first m samples were proportionally mixed with m samples generated by the generative network G to obtain a sample dataset with the size still being m. By this way, the expanded sample dataset of unqualified spot welding joints was thereby obtained, and the sample dataset size of each type of unqualified spot welding joints was the same as the sample dataset size of qualified spot welding joints.

◆ Model training

First the sample datasets of different spot welding joint quality states were normalized, for which the selected normalization Equation is:

$$x^{*} = \frac{x - x_{min}}{x_{max} - x_{min}} \tag{6}$$

Where x and x^* represent the sample value before and after normalization, respectively; x_{max} and x_{min} represent the maximum and minimum of the sample data, respectively.

The normalized sample data were then input into the AE, and the feature vectors of different spot welding joint quality states were gained after coding (i.e. Equation (7)), while the final feature vector set was obtained by combining with the feature vectors extracted based on personal experience.

$$y = f(W \cdot x + b) \tag{7}$$

Where x is the input vector denoting the normalized sample data; y is the hidden layer vector denoting the feature vector; f is the activation function; W and b constitute the network parameters set between the input layer and the hidden layer, and their meanings are connection weight and bias respectively. The selection of f, W and b are described in details in the following sections.

Finally, the feature vector set was input into the HMM, and the model parameter set of each quality state was obtained using the Baum-Welch (BW) training algorithm, denoted as $\lambda_i = (\pi_i, A_i, B_i)$, $i = 1 \sim 5$. Where, the symbol n represents the result of quality classification of spot welding joints, that is, the number of categories of classification. In this paper, spot welding joint quality can be divided into the following five categories, namely qualified joints, unfused joints, small nugget joints, cracked joints and spatter joints, so the value of n is equal to 5.

◆ Spot welding quality judgment

The monitored samples could be used for testing after the model training. In other words, the test samples and the model parameter set$\lambda_i = (\pi_i, A_i, B_i)$of each quality state were input into the Viterbi algorithm to obtain the logarithmic likelihood probability for each state, where the maximum was the state of the test samples.

4. Study of application cases

For the purpose of verifying the effectiveness of the proposed method (IGAN-AE) in judging the spot welding quality, the spot welding process of stainless steel railway carriage roof was taken as an example of study in this section. The experimental setup was first introduced and then a program written in MATLAB was employed to judge different quality states of the spot welding process. The proposed method was also compared with the existing spot welding quality judgment methods, namely GAN-AE [18], AE [23] and HMM [25].

4.1. Experimental setup

(1) Experiment description and sample data acquisition

Stainless steel roof is an important component of a stainless steel carriage body, which carries all static and dynamic loads of the railway carriage and its manufacturing accuracy also affects the assembly quality of the carriage body. Therefore, the spot welding joint samples data obtained in the spot welding process of stainless steel railway carriage roof was taken in this experiment as the object of study to explore the relationship between the data and the spot welding quality.

Fig. 6 shows a spot welding machine for roof frame, which mainly consisted of a "¬" shaped frame provided with X-axis and Y-axis. An air pressure balancer was installed below Y-axis and an electrode holder switching device was mounted at the end of the balancer. This spot welding machine was equipped with a C-shaped and an X-shaped electrode holder. The main technical parameters of the spot welding machine are listed in Table 1.

The experiment was carried out in a railway transport equipment manufacturing enterprise and the welding current I, interelectrode voltage U and electrode pressure F obtained by the spot welding machine during roof welding as well as the spot welding power calculated by the Equation $P = UI$ were taken as the objects of study to prove that the proposed improved method is feasible. The smart equipment status monitor (EM500) developed independently by the research team was adopted to monitor the welding current, interelectrode voltage and electrode pressure signals of the spot welding machine during roof welding. EM550 was installed at the output end of the spot welder's power distribution box, with the sampling frequency of current signals set as 2 ms (current value) and the acquisition time as 1 s, then 500 points could be collected within 1 s to form a sequence. The current sequence of each spot welding joint constituted a sample, and the voltage could also be analyzed similarly.

Next, a tensile test was performed on spot welding machine to test their tension-shearing strength and the nugget size. The material used in the test is SUS301L austenitic stainless steel, which was used for the roof of the railway vehicles, and its chemical composition is shown in Table 2.

The tension shearing test was carried out in accordance with the method specified in code JIS Z 2241, with the spacing between clamps also set according to the code. Specimens were fixed on a testing machine by clamps and then a tension load was applied and gradually increased until breaking so that the maximum tension-shearing load at break could be measured. In this way, the shear force on the spot welding could be calculated. The nugget size could be also measured on fractured specimens, while the entire test should be performed at room temperature. Here, only the corrugated plate-curved beam combination in the spot welding process of stainless steel roof was taken as an example for explanation. Plate name: corrugated plate + curved beam; plate thickness and combination: MT0.6 mm + ST2.0 mm. The shape of specimens is as shown in Fig. 7.

The test results were evaluated with reference to class AF criteria and specimens with the nugget size higher than the inspection threshold were deemed qualified. In addition, according to JIS Z3136, if the standard tension-shearing load was higher than the standard value of the thinnest plate in the combination, the result was considered as qualified. In this experiment, the standard value of 0.6 mm thick plate was 3.53KN. Total 11 specimens were involved in the experiment and the results are listed in Table 3. As shown in Table 3, when either the nugget size or the shear load does not meet the standard value requirement, the result is considered as disqualified.

Based on the method above, the spot welding quality can be judged as qualified or not. Meanwhile, features (nugget size, tension-shearing strength) of unqualified spot welding (unfused, small nugget, cracked, spatter) are listed in Table 4.

Table 4 shows that there are differences in nugget size and tensile strength among the four unqualified spot welding joints. In order to distinguish each kind of spot welding joint accurately, the measurement results and expert experience are combined to achieve the purpose of accurate classification.

Further, the spot welding joint samples data could be obtained for each quality state, with the results listed in Table 5. Total five sample datasets were acquired, one for qualified spot welding joints and four for unqualified spot welding joints.

(2) Experimental environment and settings of initial parameters

The computer for the experiment was configured as follows: 64-bit Windows 10, Intel Core i5, CPU 1.80 GHz, MATLAB 2014a. The initial parameters and their settings of IGAN, AE and HMM are shown in Table 6.

4.2. Experimental process and result analysis

(1) Data generation

Fig. 6. Roof frame spot welding machine.

Table 1
Main technical parameters of roof skeleton spot welding machine.

1. Input power supply: 3-phase AC, 380 ± 10%, 50 Hz;
2. Type of welding power supply: inverter power supply;
3. Capacity: 110KVA;
4. Working range: X-axis 65000 mm; Y-axis 3000 mm;
5. Working radius of welding tongs: large radius of 1500 mm; Small radius 700 mm;
6. Electrode pressure: maximum 9.8 KN;
7. "C-type welding holder": throat depth 600 mm, throat height 545 mm; any position of vertical turning $0^{\circ} \sim 90^{\circ}$;
8. "X-type welding holder": throat depth 305 mm, throat height 305 mm; any position of vertical turning $0^{\circ} \sim 15^{\circ}$.

Table 2
Chemical composition of stainless steel roof (%).

Brand	C	Mn	Si	S	P	Cr	Ni	N
SUS301L	≤0.03	≤2.00	≤1.00	≤0.03	≤0.45	16.00 ~ 18.00	6.00 ~ 8.00	≤0.20

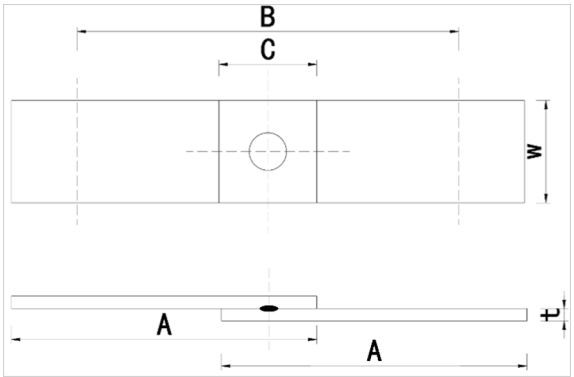

Fig. 7. Shape of specimen.

Table 3
Test results of stainless steel roof (automatic welding tongs).

Serial number	Material combination	Nuggetsize (mm)	Standard values (mm)	Shear load (KN)	Standard values (KN)	Conclusion
1	MT0.6 + ST2.0	5.1	3.3	9.73	3.53	qualified
2		1.7		2.54		unqualified
3		2.9		4.04		unqualified
4		6.2		8.41		qualified
5		3.7		4.86		qualified
6		4.8		5.50		qualified
7		5.9		6.76		qualified
8		6.1		7.17		qualified
9		6.3		7.66		qualified
10		5.5		6.54		qualified
11		6.0		6.97		qualified

Table 4
Characteristic description of unqualified spot welding joints.

Name of spot welding joint	Characteristic description Nugget size (mm)	Shear load (KN)
unfused	no nugget or minimum size	very low
small nugget	small	low
cracked	smaller size	slightly less than standard value
spatter	size close to standard values	lower

Table 5
Description of spot welding joint sample data set.

Spot welding joint data set		Number of samples
Spot welding joints of qualified quality		1000
Spot welding joints of unqualified quality	unfused	30
	small nugget	80
	cracked	120
	spatter	60

Table 6
The settings of initial parameters of IGAN, AE, HMM.

Models	Initial parameters and settings
IGAN	Random noise: $z \sim N(0, var(\cdot))$; Generating network training method: Adam algorithm; Learning rate: 0.0002;Number of iterations: 2000;Discriminant network optimization method: stochastic gradient descent method
AE	Number of layers: 5; Number of input nodes: 500, output nodes: 5, hidden layer nodes: 100; Initial weight matrix $_W$ and bias vector $_b$: random initialization; Learning rate: 0.01
HMM	State transition diagram: 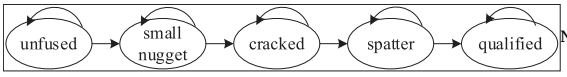 Number of hidden states: $_{N=5}$; observation states $_M$; Initial probability vector: $\pi_0 = [1\ 0\ 0\ 0\ 0\ ]$; Initial state transition matrix:$A_0 = \begin{bmatrix} a_{11} & a_{12} & 0 & 0 & 0 \\ 0 & a_{22} & a_{23} & 0 & 0 \\ 0 & 0 & a_{33} & a_{34} & 0 \\ 0 & 0 & 0 & a_{44} & a_{45} \\ 0 & 0 & 0 & 0 & a_{55} \end{bmatrix} = \begin{bmatrix} 0.5 & 0.5 & 0 & 0 & 0 \\ 0 & 0.5 & 0.5 & 0 & 0 \\ 0 & 0 & 0.5 & 0.5 & 0 \\ 0 & 0 & 0 & 0.5 & 0.5 \\ 0 & 0 & 0 & 0 & 1 \end{bmatrix}$ Observation symbol matrix: $B_0 = \begin{bmatrix} b_{11} & b_{12} & \cdots & b_{1n} \\ b_{12} & b_{22} & \cdots & b_{2n} \\ b_{31} & b_{32} & \cdots & b_{3n} \\ b_{41} & b_{42} & \cdots & b_{4n} \\ b_{51} & b_{52} & \cdots & b_{5n} \end{bmatrix}$ The maximum number of iterations: 500;Convergence error:1e-8.

As indicated in Table 5, the number of qualified spot welding joint samples obtained in the experiment was much more than the number of unqualified ones, which formed an unbalanced dataset. In addition, the AE algorithm needed a large number of data to train the model parameters, so expanding the sample dataset of unqualified spot welding joints was necessary. Specific steps are as follows:

Step1. Curves of four kinds of unqualified spot welding joint samples (unfused, small nugget, cracked, and spatter) were obtained in the process of welding, including welding current, interelectrode voltage, electrode pressure and welding power. The Equation $P = UI$ was used to calculate the welding power.

Step2. The curves above were sampled at set frequencies. For example, the sampling frequency of welding current signals was set as 2 ms, so 500 data points could be sampled within 1 s to form a sequence. All acquired current sequences of each spot welding joints constituted a sample. This step was also performed for other curves in a similar way.

Step3. The MATLAB function $var(\cdot)$ was used to calculate the variance of each sample.

step4. For random noise, $normpdf(range\ of\ the\ variable\ value, 0, var(\cdot))$ was employed to generate normally distributed data z.

Step 5. The generative network $G(z)$ was adopted to generate the noise data sample.

Step6. The real sample was mixed with the noise sample at the ratio $(1\text{-}\alpha):\alpha$ to generate a mixed sample.

Step7. The discriminant network D was used to judge if the mixed sample was similar to the real sample.

Then the samples of each kind of unqualified spot welding joint could be acquired by repeating Step5 ~ Step7, realizing the purpose of expanding the sample dataset.

Furthermore, a standard GAN [24] was introduced in this paper to compare with the IGAN regarding the data generation effects. In order to comprehensively compare the generated signals (including the original curves of welding current, normally distributed random noise, curves of the mixed sample, curves of the samples generated by IGAN and GAN), the curves corresponding to each kind of unqualified spot welding joint samples are shown in Fig. 8~Fig. 11. Curves of samples with unfused, small nugget, cracked and spatter are shown in Figs. 8, 9, 10 and 11, respectively. It shall be pointed out that the mixing proportion coefficient α plays an important role in the IGAN algorithm, whose value is determined experimentally. It was found by experiments that when $\alpha = 0.3$, namely the noise data and the real data accounted for 30% and 70%, respectively, the quality of the generated unqualified spot welding joint samples achieved the purpose of the improved standard GAN algorithm mentioned above, so the value of α was set to 0.3.

As shown in Fig. 8, both IGAN and GAN can generate samples with the curves similar to those of real sample data, but differences still exist between them, which are analyzed as follows.

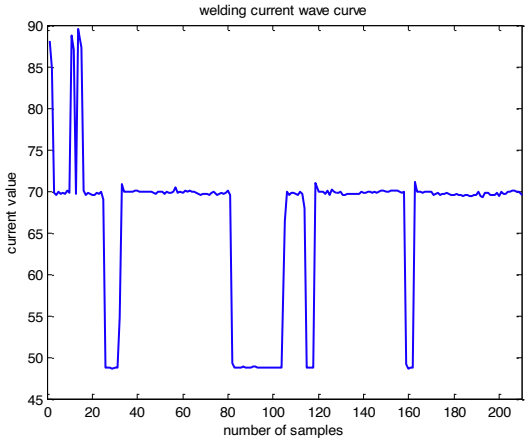

(a) welding current wave cure

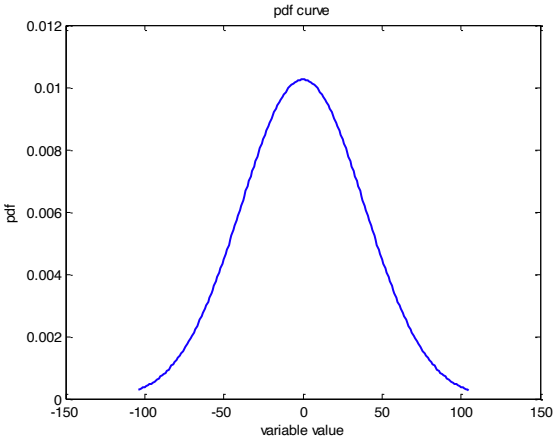

(b) pdf curve of random noise data

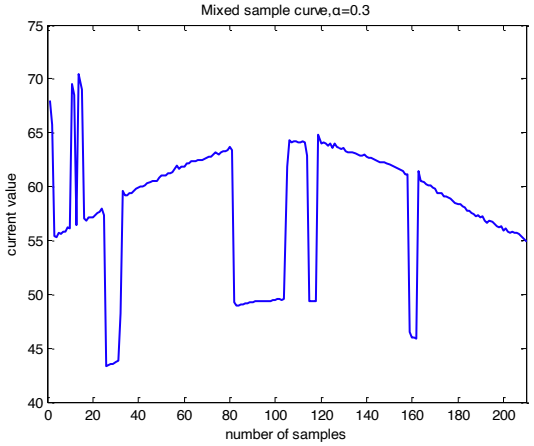

(c) mixed sample curve, α=0.3

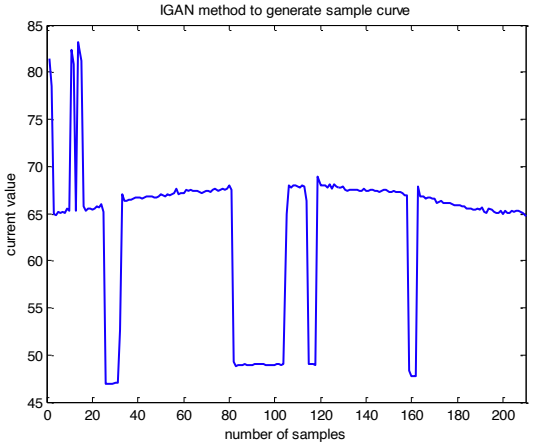

(d) IGAN method to generate sample curve

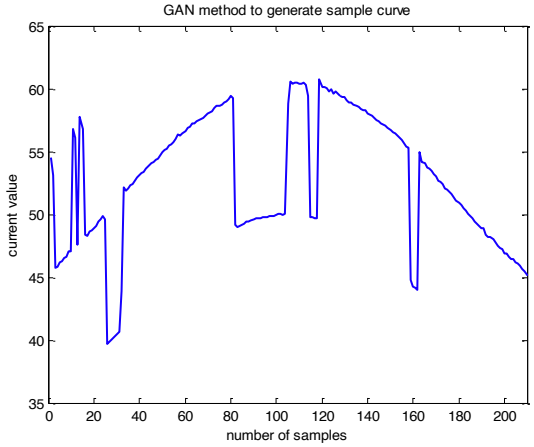

(e) GAN method to generate sample curve

Fig. 8. Unfused joint waveform curve of unqualified quality.

◆ The original curve of welding current is shown in Fig. 8(a), which is smooth with no obvious oscillation and less glitches. Fig. 8 (b) shows the probability density function graph (normally distributed) of random noise data with the average being 0, the variance calculated using the function var(·), and the data dimension unchanged. Fig. 8(c) shows the curve of the mixed sample ($\alpha = 0.3$), which is no longer smooth, and shows rise and decline, with the declining rate higher than the rising rate. Meanwhile,

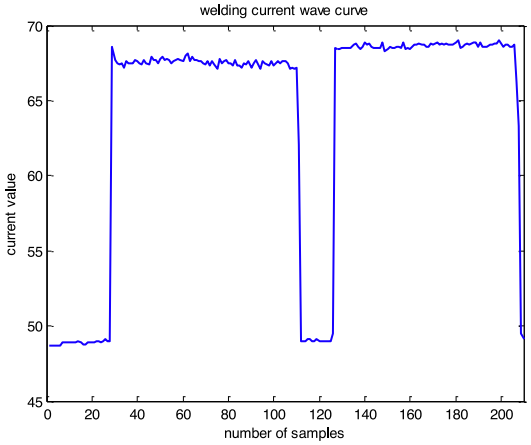

(a) welding current wave curve

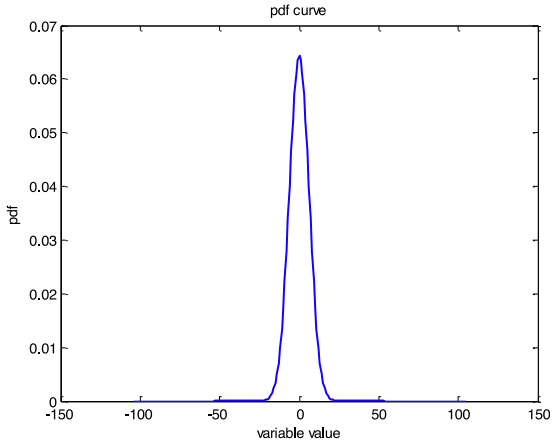

(b) pdf curve of random noise data

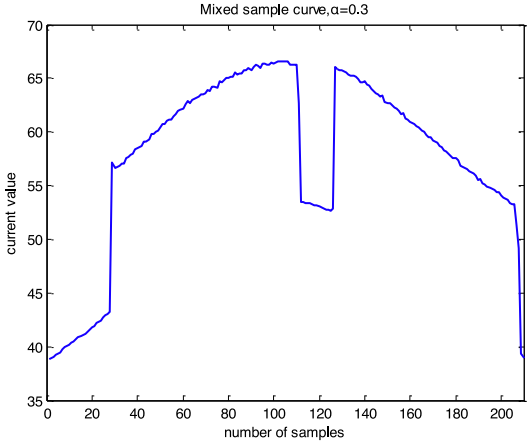

(c) mixed sample curve, α=0.3

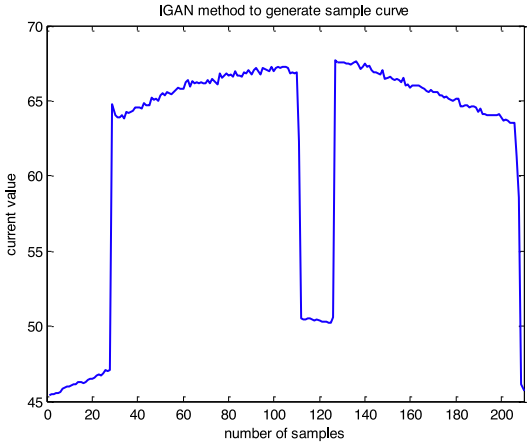

(d) IGAN method to generate sample curve

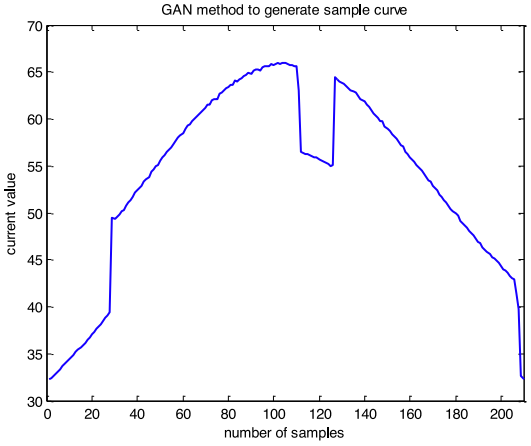

(e) GAN method to generate sample curve

Fig. 9. Small nugget joint waveform curve of unqualified quality.

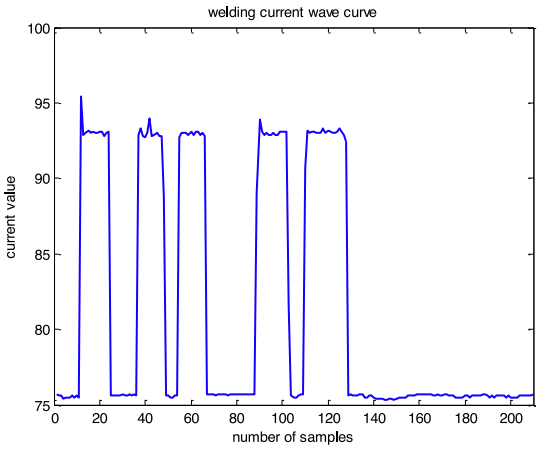

(a) welding current wave curve

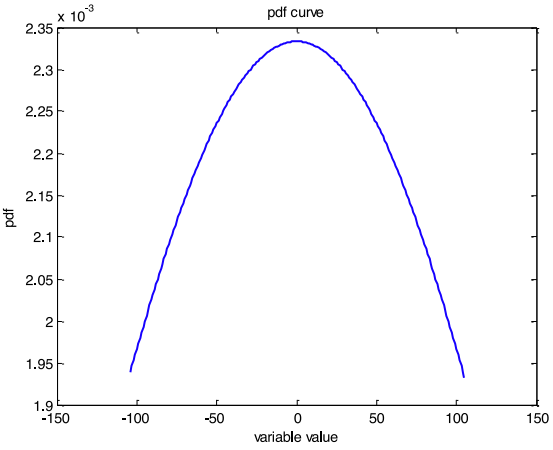

(b) pdf curve of random noise data

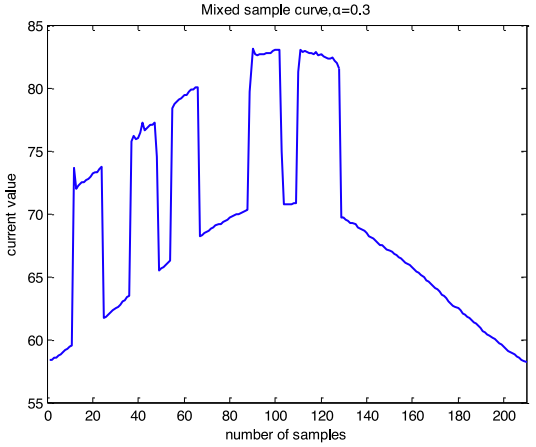

(c) mixed sample curve,α=0.3

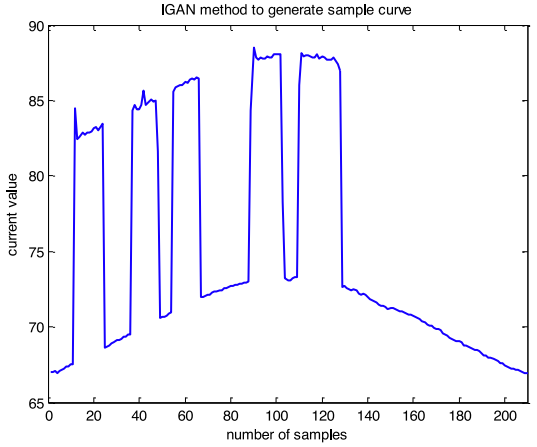

(d) IGAN method to generate sample curve

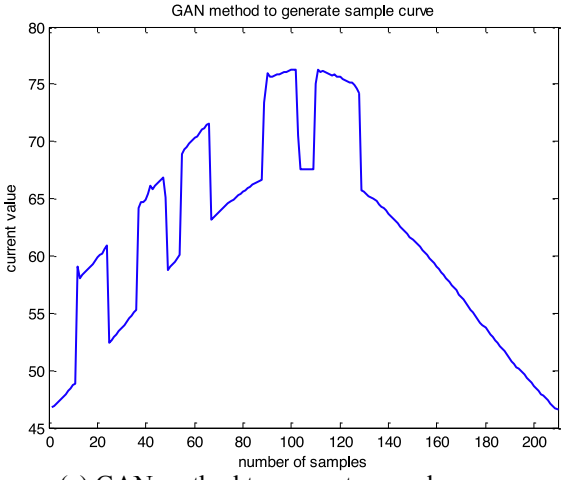

(e) GAN method to generate sample curve

Fig. 10. Cracked joint waveform curve of unqualified quality.

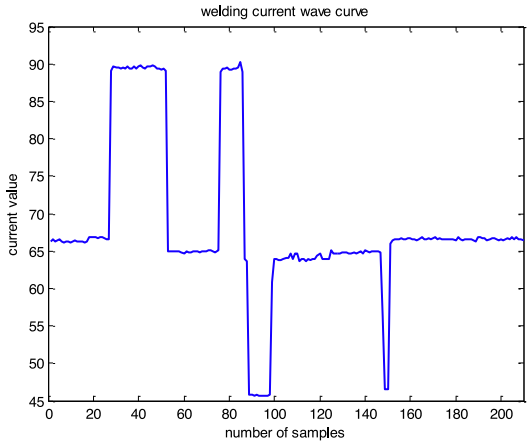

(a) welding current wave cure

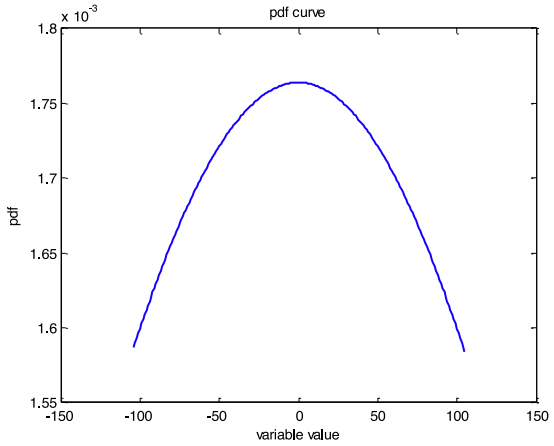

(b) pdf curve of random noise data

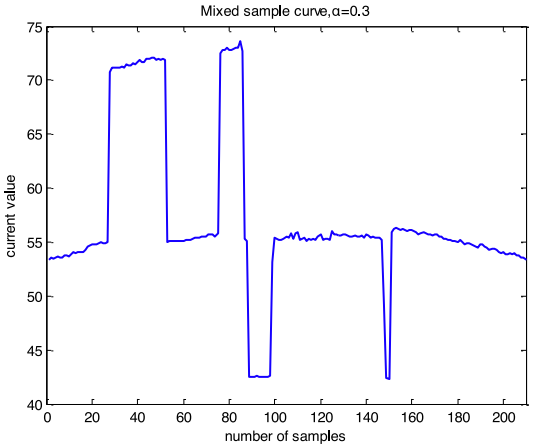

(c) mixed sample curve,α=0.3

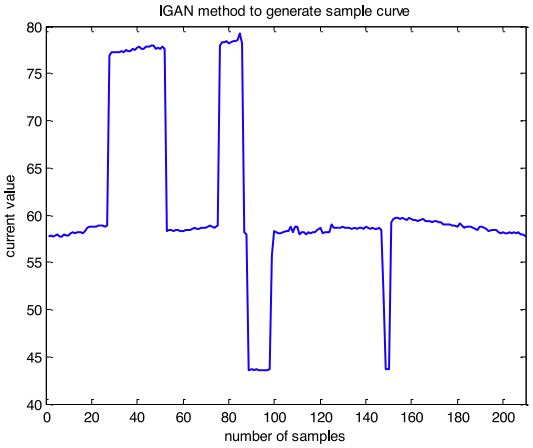

(d) IGAN method to generate sample curve

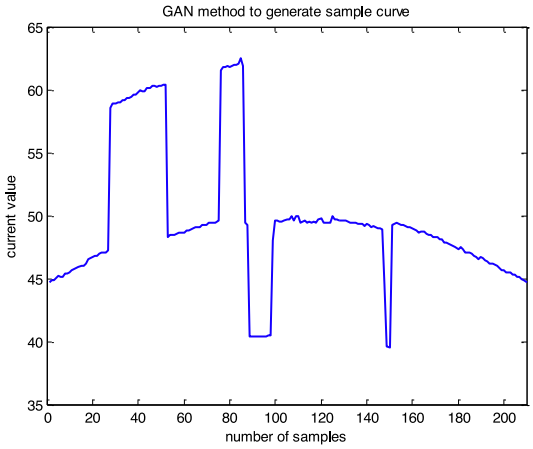

(e) GAN method to generate sample curve

Fig. 11. Spatter joint waveform curve of unqualified quality.

the glitches are still less. Fig. 8(d) displays the curve of the sample generated by IGAN, which is smooth, but shows minor rise and decline. The glitches are still less. Fig. 8(e) displays the curve of the sample generated by GAN, which is not smooth and shows major rise and decline. However, the glitches are still less.

- The comparison among Fig. 8 (a), (c), (d) and (e) manifests IGAN can keep the curve shape of original current better because of a large portion of real data in the mixed sample. A large change is detected on the curve of the sample generated by GAN due to the fact that the random noise did not simulate the real data satisfactorily.

As can be seen from Fig. 9, either IGAN or GAN can generate sample data and maintain the features of real sample data to a certain extent, but differences still exist between them:

- The original curve of welding current is shown in Fig. 9(a) and a large oscillation is noticed in its early period, while the curve becomes very smooth in its middle to late period with less glitches. Fig. 9(b) shows the probability density function graph (normally distributed) of random noise data with the average being 0, the variance calculated using the function var(·), and the data dimension unchanged. Fig. 9(c) shows the curve of the mixed sample data of ($\alpha = 0.3$), which demonstrates a considerable oscillation in its early period, a certain level of rise in its early to middle period, a short-term smooth section in its middle period and a certain level of decline in its late period, while less glitches are detected. Fig. 9(d) displays the curve of the sample generated by IGAN, which also demonstrates a considerable oscillation in its early period, but a minor rise in its early to middle period and a minor decline in its middle to late period. The glitches are still less. Fig. 9(e) displays the curve of the sample generated by GAN, which demonstrates a considerable oscillation in its early period, a major rise in its early to middle period and a major decline in its middle to late period. However, the glitches are still less.
- The comparison among Fig. 9 (a), (c), (d) and (e) manifests the data acquired by IGAN approximate to the real sample data in a satisfied way, while a poor fitting result is noticed for GAN. The cause lies in that the real sample data play a leading role in the mixed sample and the features of real sample data are better inherited.

According to Fig. 10, sample data that are close to the real sample data can be generated by either of the methods, but differences still exist between them.

- The curve of welding current with less glitches is shown in Fig. 10(a), which is smooth in its early and late period, but a sharp decline occurs in its middle period. Fig. 10(b) shows the probability density function graph (normally distributed) of random noise data with the average being 0, the variance calculated using the function var(·), and the data dimension unchanged. Fig. 10(c) shows the curve of the mixed sample ($\alpha = 0.3$), which is generally smooth with minor rise and decline noticed in its early and late periods. However, a major decline is observed in its middle period. Nevertheless, the glitches are still less. Fig. 10 (d) displays the curve of the sample generated by IGAN, which is generally smooth in its early and late periods, but a sharp decline is observed in its middle period. The glitches are still less. Fig. 10(e) displays the curve of the sample generated by GAN, which demonstrates a major rise in its early period, a major decline in its late period and a sharp decline in its middle period. However, the glitches are still less.
- The comparison among Fig. 10 (a), (c), (d) and (e) manifests the curve of the sample generated by IGAN is better than that generated by GAN, indicating the mixed sample can maintain the features of real sample data better.

As shown in Fig. 11, the sample data generated by either of the methods can better approximate to the real sample data, but differences still exist among them.

- The curve shown in Fig. 11(a) is generally smooth with less glitches, while a certain level of oscillation is noticed on the whole curve, with the oscillation in its early period more intensive than that in its middle and late periods. Fig. 11(b) shows the probability density function graph (normally distributed) of random noise data with the average being 0, the variance calculated using the function var(·), and the data dimension unchanged. The curve in Fig. 11(c) has less glitches and shows a certain level of rise with minor oscillation in its early and middle periods, and a major decline in its late period. The curve in Fig. 11(d) has less glitches and shows a minor rise with a certain level of oscillation in its early and middle periods, and a certain level of decline in its late period. The curve in Fig. 11(e) also has less glitches but shows a major rise with minor oscillation in its early and middle periods, and a sharp decline in its late period.
- The comparison among Fig. 11 (a), (c), (d) and (e) manifests the curve of the sample generated by IGAN is better than that generated by GAN, indicating the mixed sample can maintain the features of real sample data better.

To sum up, the sample generation method presented in this paper is better than GAN in the stability of generated sample data, as the generated sample can approximate to real sample data very well.

Fig. 12 compares the number of original samples and that of generated samples, with only the welding current taken as an example here for illustration. The results demonstrate that: the number of qualified spot welding joint samples obtained in the experiment is much more than the number of unqualified ones; using the IGAN method to generate unqualified spot welding joint samples (all close to qualified spot welding joint samples) can largely expand the sample data set, but the number of generated unqualified spot welding joint samples varies. This suggests that the IGAN method guarantees the quantity of generated samples to some extent, but there is no completely guaranteed for their quality.

(2) Model training

◆ Feature selection

As described above, the IGAN algorithm was used to generate the sample data of unqualified spot welding joints (unfused, small nugget, cracked and spatter), which increased the number of unqualified spot welding joint samples and made it roughly equal to the number of qualified spot welding joint samples. A total of 5,000 samples (1,000 for each type of spot welding joints) were obtained, and 80% of the samples from each type of spot welding joints were randomly selected to be used as the training set, and the remaining 20% is used as the test set, that was, 800 training samples and 200 test samples were available for each type of spot welding joints.

AE and personal experience were combined in this paper to get the feature vector of each type of spot welding joints, for which the steps are shown in Table 7. Finally, a total of 11 features closely related to the spot welding quality were obtained, namely the welding current I, the first-order difference ΔI and the integral value; the interelectrode voltage U, the first-order difference ΔU, the integral value and the variance; the electrode pressure F, and the first-order difference ΔF; the powe rP and the first-order differenceΔP.

◆ Training of HMM model parameters

The initial model parameters$\lambda_0 = (\pi_0, A_0, B_0)$ of HMM and the feature vector sets of the five spot welding joint quality states were input into the BW algorithm for parameter training to obtain the model parameters $\lambda_i = (\pi_i, A_i, B_i), i = 1, 2, \cdots, 5$ corresponding to each state. The dimension of the observation symbol matrix B_0 was $5 * 11$, and the initial values of the matrix were generated by averaging, that was, the value of each element in the matrix was approximately 0.091. Table 8 exhibits the logarithmic likelihood probabilities calculated by the Viterbi algorithm when the test data were input into the above models, in which the boldface represents the maximum likelihood probabilities calculated from each model.

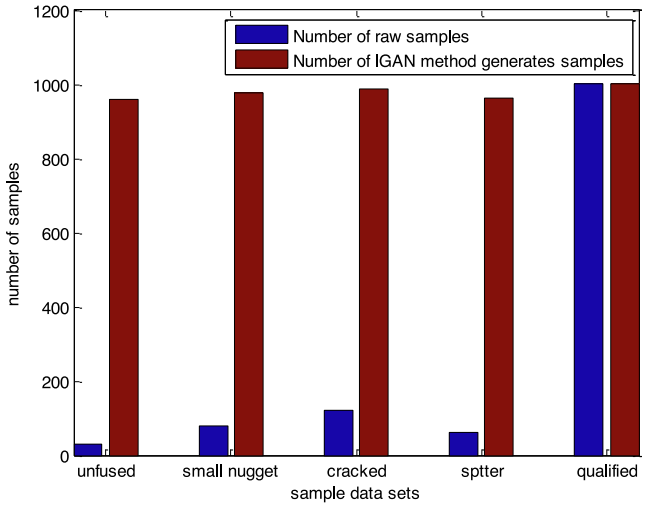

Fig. 12. Comparison of sample number of spot welding joints.

Table 7
Feature extraction of welding samples.

Input: sample data of each type of spot welding joints and model parameters

Output: feature vector of each type of spot welding joints

Step 1. Use Equation (6) to process the sample dataset and obtain x^*;

Step 2. Take x^* as the input, adopt the gradient descent based optimization method and the minimization Equation (8) for training to gain the network parameters θ_1 of the first layer, and calculate the output h_1 of the first hidden layer.

$$minJ = \frac{1}{N}\|y_0 - Y_0\|^2 \tag{8}$$

Where, θ_1 represents the set of network parameters W_1 (connection weight) and b_1 (bias) between the input layer and the hidden layer, and $\theta_1 = \{W_1, b_1\}$ can be initialized by the Equations $W_1 = rand(N, M-1)$ and $b_1 = zeros(N, 1)$. In the Equation, the symbol$N$ is the number of samples, while$M$ is the characteristic component of each sample. In this paper, the values for N and M are set to 1000 and 11, respectively. y_0 is the actual output; and Y_0 is the ideal output.

Step 3. Take the output parameter h_1 of the first hidden layer as the input of the second layer, and repeat the process to get the parameter θ_2 of the second layer, meanwhile, calculate the output parameter h_2 of the second hidden layer;

Step 4. Repeat Steps 1 and 2 for layer-by-layer training to obtain the weight parameters$\theta_1, \cdots, \theta_5$ and the outputh_5 of the fifth hidden layer;

Step 5. Calculate the welding current I, interelectrode voltage U, electrode pressure F, and power Pas well as their first-order differencesΔI,ΔU, ΔF and ΔP, total eight features;

Step 6. Combine the feature vectors from Steps 3 and 4 together to gain the feature vector set of each weld joint quality state.

Table 8
Log-likelihood probability value of HMM classification method.

States	Models unfused joint	small nugget joint	cracked joint	spatter joint	qualified joint
unfused	**−55.2234**	−56.6070	−93.2108	−89.0983	−62.7034
small nugget	−90.7362	**−47.1276**	−56.3493	−81.6180	−77.3441
cracked	−72.8276	−97.7610	**−44.2858**	−53.2112	−64.2491
spatter	−85.9310	−69.3859	−62.8935	**−38.6332**	−47.1399
qualified	−60.6226	−90.3314	−67.6271	−74.1755	**−52.9696**

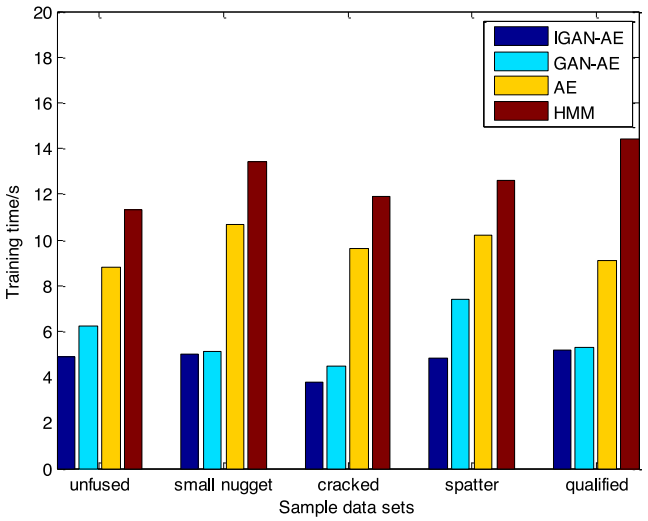

Fig. 13. Comparison of training time of different classification methods.

GAN-AE, AE and HMM were introduced in this paper for comparison, of which the initial parameter settings were consistent with Table 6, and the classifier for GAN-AE and AE was soft-max. The proposed four spot welding quality judgment methods are compared below in terms of the model training time, test time and classification accuracy.

Fig. 13 compares the training time of the four methods. As can be seen, for the five training sample datasets, the training times of IGAN-AE and GAN-AE are significantly less than that of AE and HMM, while the training time of AE is less than HMM; the training time of IGAN-AE is slightly different from that of GAN-AE (almost the same for the sample datasets of small nugget and qualified), but for the sample datasets of unfused, cracked and spatter, IGAN-AE is notably better than GAN-AE, reflecting that IGAN-AE trains faster than GAN-AE. This analysis demonstrates that,

- The IGAN-AE method not only ensures the diversification of generated samples, but also reduces the generation of irrelevant samples. Moreover, the feature extraction method based on AE and personal experience enhances the efficiency of feature extraction to a certain extent.
- The training of IGAN-AE, GAN-AE and AE are all faster than that of HMM, indicating that the samples processing efficiency of traditional mode classification methods is obviously affected when processing large datasets.

Fig. 14 compares the time consumed by different classification methods on the test datasets for spot welding quality estimation. As can be seen, the IGAN-AE method is the most time-saving in estimating the welding quality, followed by GAN-AE, AE and HMM in order. This manifests that the IGAN-AE method outperforms the other three methods regarding both the quality of generated sample data and the accuracy of feature selection.

To further prove the effectiveness of the method proposed above, 1,000 samples (200 for each of unfused, small nugget, cracked, spatter and qualified joints) were selected and tested, and the obtained confusion matrix of each classification method is given in Table 9.

As indicated in Table 9, all of the four classification methods can judge spot welding quality with high classification accuracy, but misclassification occurs in all the methods; moreover, the classification accuracy is varying for the four methods, as the element values on the main diagonal of IGAN-AE's confusion matrix are all higher than those of the other three methods, which are ranked as GAN-AE $>$ AE $>$ HMM. This evidences the better classification accuracy of IGAN-AE than the other three methods. In addition, according to Table 8, the logarithmic likelihood probability for the test samples in each spot welding quality state is close to the maximum logarithmic likelihood probability in that state, indicating the significant classification effect of this method.

In conclusion, the IGAN-AE method consumes the model training time and the sample testing time slightly less than GAN-AE, but

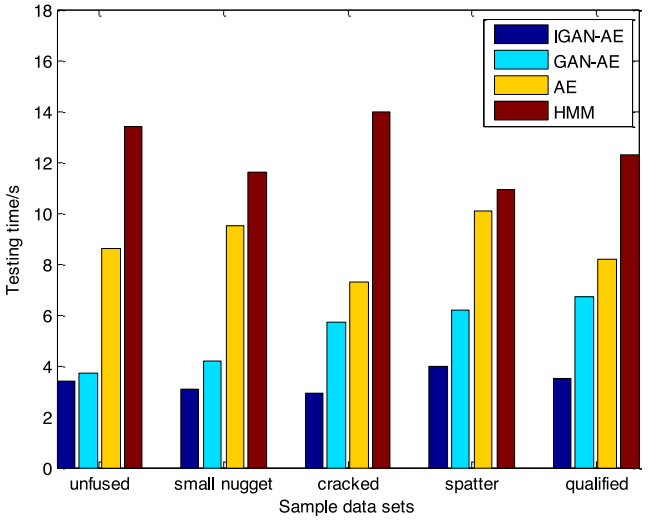

Fig. 14. Comparison of testing time of different classification algorithms.

Table 9
Confusion matrix of different classification methods.

IGAN-AE

	unfused	small nugget	cracked	spatter	qualified
unfused	186	10	3	0	1
small nugget	4	196	0	0	0
cracked	6	3	190	1	0
spatter	1	0	4	194	1
qualified	0	6	0	6	188

GAN-AE

	unfused	small nugget	cracked	spatter	qualified
unfused	174	10	1	13	2
small nugget	9	180	1	9	1
cracked	3	11	185	0	1
spatter	0	8	8	184	0
qualified	1	7	2	1	189

AE

	unfused	small nugget	cracked	spatter	qualified
unfused	171	9	1	18	1
small nugget	15	165	0	16	4
cracked	17	19	158	4	2
spatter	7	9	8	170	6
qualified	8	8	16	3	173

HMM

	unfused	small nugget	cracked	spatter	qualified
unfused	155	28	1	12	4
small nugget	20	154	5	19	2
cracked	9	14	158	16	3
spatter	14	15	13	145	13
qualified	12	13	9	15	151

remarkably less than AE and HMM; in addition, the IGAN-AE method outperforms GAN-AE, AE and HMM in classification accuracy, which reflects that the overall performance of the model has been improved to a certain extent, and also verifies the effectiveness of the proposed method.

5. Conclusions

An method for judging the spot welding quality based IGAN and AE was proposed in this paper, which integrated IGAN and AE to construct a network structure having the functions of sample generation, feature extraction and pattern recognition. The main innovation of this study was that the proposed method could judge the spot welding quality in the context of small sample training. The spot welding data of stainless steel roof was used in this paper as the original data for experimental study, and the results demonstrated that:

- IGAN method not only has the ability to generate sample data, but also ensures that the generated data can fit the waveform curve of spot welding joint samples with unqualified quality as far as possible.
- Compared with IGAN-AE, AE and HMM, the time spent by IGAN-AE on the training datasets and on the test datasets is shorter.
- IGAN-AE's classification accuracy is also higher than IGAN-AE, AE and HMM.

Therefore, the proposed method is feasible and effective when applied to judge the quality of spot welding joints based on a small sample dataset.

CRediT authorship contribution statement

Bing Wang: Conceptualization, Methodology, Software, Data curation, Writing – original draft, Writing - review & editing.

Declaration of competing interest

The authors declare that it has no known competing personal relationships or financial interests that could have appeared to influence the work reported in this paper.

References

[1] L. Gong, Realtime monitoring, control and quality assessment of the resistance welding, Doctoral Dissertation of Shanghai Jiaotong University. (2009).
[2] P. Podržaj, I. Polajnar, J. Diaci, Z. Kariž, Overview of resistance spot welding control, Sci. Technol. Weld. Joining 13 (3) (2008) 215–224.
[3] K. Zhou, P. Yao, Overview of recent advances of process analysis and quality control in resistance spot welding, Mech. Syst. Sig. Process. 124 (2019) 170–198.
[4] M. Kimchi, D.H. Phillips, Resistance Spot Welding: Fundamentals and Applications for the Automotive Industry, Mechanical Engineering. 1–129 (2017).
[5] A.M. Al-Mukhtar, Review of resistance spot welding sheets: Processes, and Failure Mode, Advanced Engineering Forum. 17 (2016) 31–57.
[6] H.M. Mallaradhya, K.M. Vijay, R. Ranganatha, RESISTANCE SPOT WELDING: A REVIEW, International Journal of Mechanical and Production. 8 (2) (2018) 403–418.
[7] P. X. Zhang, Z. F. Zhang, J. H. Chen, Online Diagnosis of Joints Quality in Resistance Spot Welding for Sedan Body, International Conference on Robotic Welding, Intelligence and Automation, RWIA 2014: Robotic Welding, Intelligence and Automation. (2014) 263-272.
[8] Z.J. Mo, Y.B. Fan, M.Z. Peng, Inspection Method of Welding Quality about Power Battery Based on 3D Machine Vision, Mechanical&Electrial Engineering Technology. 49 (04) (2020) 1–3.
[9] X.K. Wang, S.Y. Guan, L. Hua, B. Wang, X.M. He, Classification of spot-welded joint strength using ultrasonic signal time-frequency features and PSO-SVM method, Ultrasonics 91 (2019) 161–169.
[10] H.T. Hoseini, M. Farahani, M. Sohrabian, Process analysis of resistance spot welding on the Inconel alloy 625 using artificial neural networks, Int. J. Manuf. Res. 12 (4) (2017) 444, https://doi.org/10.1504/IJMR.2017.088398.
[11] D.-C. Anghel, A. Ene, L. Slătineanu, V. Merticaru, A.M. Mihalache, O. Dodun, M.I. Ripanu, G. Nagit, M. Coteata, M. Boca, R. Ibanescu, C.E. Panait, Study of the influence of the technological parameters on the weld quality using artificial neural networks, MATEC Web of Conferences. 178 (2018) 03011, https://doi.org/10.1051/matecconf/201817803011.
[12] S.J. Chen, N. Wu, J. Xiao, T.M. Li, Z.Y. Lu, Expulsion Identification in Resistance Spot Welding by Electrode Force Sensing Based on Wavelet Decomposition with Multi-Indexes and BP Neural Networks, Applied Sciences. 9 (19) (2019) 4028.
[13] J. Park, K.-Y. Kim, Evaluation of interval regression analysis for uncertain resistance spot welding quality data, Int. J. Comput. Integr. Manuf. 31 (8) (2018) 760–768.
[14] J. Yu, Quality estimation of resistance spot weld based on logistic regression analysis of welding power signal, Int. J. Precis. Eng. Manuf. 16 (13) (2015) 2655–2663.
[15] D. Zhao, Y. Wang, D. Liang, M. Ivanov, Performances of regression model and artificial neural network in monitoring welding quality based on power signal, J. Mater. Res. Technol. 9 (2) (2020) 1231–1240.
[16] B. Wang, A study on spot welding quality judgment based on hidden Markov model, Proceedings of the Institution of Mechanical Engineers Part E-Journal of Process Mechanical Engineering. 235(2) (2020)208-218.
[17] B. Wang, P. Yan, Q. Zhou, L.B. Feng, State recognition method for machining process of a large spot welder based on improved genetic algorithm and hidden Markov model, Proceedings of the Institution of Mechanical Engineers, Part C: Journal of Mechanical Engineering Science. 231 (11) (2017) 2135–2146.
[18] J. Gu, K.S. Zhang, Y.M. Zhu, Research on weld defect image classification based on convolutional neural network, Journal of Applied Optics. 41 (3) (2010) 531–537.
[19] X.F. Huang, Deep transfer learning for online welding quality monitoring, Degree thesis of, Guangxi University, 2019.
[20] X. Xiong, H. K. Jiang, X. Q. Li, M. G. Niu, A Wasserstein gradient-penalty generative adversarial network with deep auto-encoder for bearing intelligent fault diagnosis, Measurement Science and Technology. 31(4)(2019).
[21] Y.-R. Wang, G.-D. Sun, Q.i. Jin, Imbalanced sample fault diagnosis of rotating machinery using conditional variational auto-encoder generative adversarial network, Appl. Soft Comput. 92 (2020) 106333, https://doi.org/10.1016/j.asoc.2020.106333.
[22] I. Chakraborty, R. Chakraborty, D. Vrabie, Generative adversarial network based autoencoder: application to fault detection problem for closed loop dynamical systems, Machine Learning. 1–9 (2018).
[23] Y. Zhang, D. You, X. Gao, C. Wang, Y. Li, P.P. Gao, Real-time monitoring of high-power disk laser welding statuses based on deep learning framework, J. Intell. Manuf. 31 (4) (2020) 799–814.
[24] I. Goodfellow, J. Pouget-Abadie, M. Mirza, B. Xu, D. Warde-Farley, S. Ozair, A. Courvile, Y. Bengio, Generative adversarial nets, Advances in Neural Information Processing Systems. (2014) 2672–2680.
[25] B. Wang, Study on spot welding quality judgement based on hidden Markov model, Doctoral dissertation of Chongqing University. (2018).